Journal of Engineering Physics and Thermophysics, Vol. 84, No. 4, July, 2011

SIMULATION OF THE SUPERSONIC TURBULENT FLOW AROUND A CYLINDER WITH COAXIAL DISKS

S. A. Isaev,[a] Yu. M. Lipnitskii,[b] A. N. Mikhalev,[c] A. V. Panasenko,[b] and A. E. Usachov[d]

UDC 532.517:4

The turbulent axisymmetric flow around a stepped body — a cylinder with coaxial front and rear disks — has been calculated with the aid of a VP2/3 package based on multiblock computational technologies and the generalized procedure of pressure correction. The computational model has been tested with the example of a supersonic flow around a sphere. The numerical forecasts made with the use of Spalart–Allmares shear stress transfer and eddy viscosity transfer models have been compared with the data of the aeroballistic experiment, wind tunnel tests, and the results of the calculation of the flow around the disk–cylinder arrangement by a simplified zonal model in a wide range of variation of the incident flow Mach number (from 1.5 to 4). We have obtained a good agreement between the calculated transverse flow density distributions in the front stalling zone and those determined from the interferograms for the wave-drag-rational disk–cylinder arrangement. The influence of the rear disk on the drag of the disk–cylinder–disk arrangement has been estimated.

Keywords: *decrease in the motive drag, stepped bodies, supersonic flow, turbulence, shock wave, calculation, multiblock computational technologies, Menter model, Spalart–Allmaras model, aeroballistic experiment, wind tunnel tests.*

Introduction. Twenty to thirty-five years ago, the supersonic flow around stepped bodies received much attention from aerodynamicists. The P. Chang [1] method for decreasing the wave drag of a blunt body connected with placing a thin needle in front of it led sometimes to unstable detached flow conditions and hysteresis phenomena which could only be avoided, as it turned out, by placing a small-diameter disk at the point of the needle [2]. Fixing the flow separation point made it possible to create a fairly stable front separation zone (FSZ) and considerably decrease the load on the front part of the body [3]. At first it seemed that the nonviscous gas flow model (the solution of Euler equations by the Godunov method) would be acceptable for describing the flow in the FSZ [4–7]. However, for optimal values of the disk diameter and its position in front of the body, wide differences between numerical forecasts and available experimental data on the wave drag were revealed. In the early 1980s, a fundamental result on the influence of the type of computational mesh on the motion drag of the disk-cylinder configuration was obtained from the viewpoint of the nonviscous gas flow model, and a significant effect of the artificial diffusion mechanism was shown [8]. The development of a zonal model in which a suspended shear layer is introduced into the FSZ and the Reynolds equations with a closure by the Prandtl turbulence model are solved in its limits made it possible to bring the forecasts of integral and local force characteristics closer to experimental data [9, 10]. However, certain discrepancies were noted between calculated and experimental density fields obtained in flight tests on the aeroballistic route, which were supposed to be overcome by using differential turbulence models [11]. Fairly not long ago, in the Vortex-Cell 2050 project, the multiblock computational technologies [12] and the widely used Menter [13, 14] shear stress transfer model corrected with account for the influence of the curvature of streamlines that are developed within the framework of the approach based on the pressure correction procedure were generalized to the case of compressible viscous gas flows in the presence of shock waves [15]. In a series of methodological calculations, a numerical simulation of the hypersonic air flow around a plate upon interaction of the incident oblique shock wave with the separat-

[a]St. Petersburg State University of Civil Aviation, 38 Pilotov Str., St. Petersburg, 196210, Russia; [b]TsNII of Machine Building, 4 Pionerskaya Str., Korolev, Moscow Region, 140070, Russia; [c]A. F. Ioffe Physical-Technical Institute, 26 Politekhnicheskaya Str., St. Petersburg, 194021, Russia; [d]Branch FGUP TsAGI, 17 Radio Str., Moscow, 105005, Russia; email: isaev3612@yandex.ru. Translated from Inzhenerno-Fizicheskii Zhurnal, Vol. 84, No. 4, pp. 764–776, July–August, 2011. Original article submitted October 15, 2010.

1062-0125/11/8404-0827

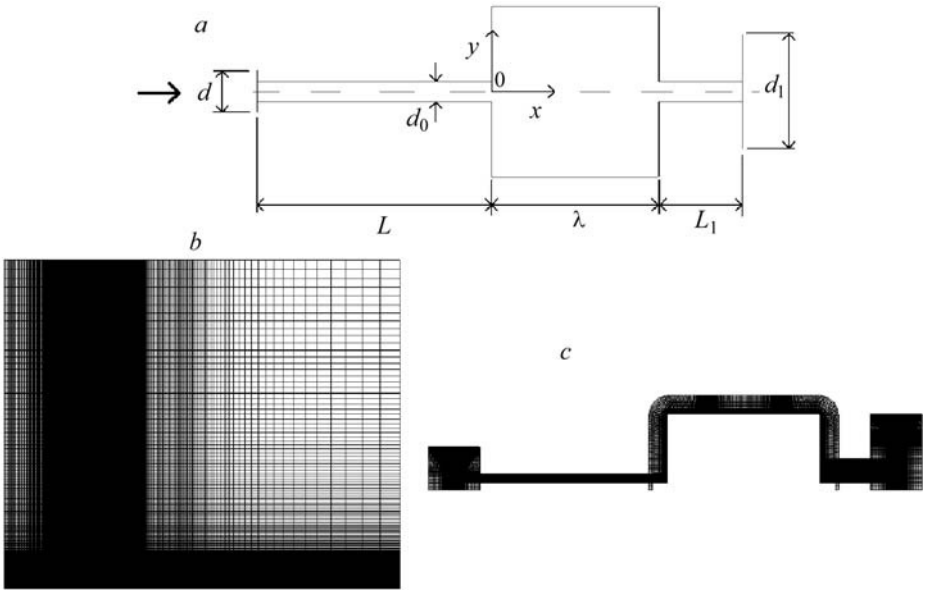

Fig. 1. Contours of the stepped body model — a cylinder with protruding front and rear coaxial disks (a), Cartesian computational grid (b), O-type curvilinear computational grid and four cylindrical fragments of the multiblock computational grid (c).

ing shear layer and the supersonic flow around the compression angle (comparison with Horstsmann's experiment) was carried out [16]. The supersonic flows around a circular cylinder, a sphere, and a sharp- and a blunt-nose cones (tunnel experiments of the TsAGI and the IM MGU, aeroballistic experiment in the Van Dyke atlas), as well as around a drop-shaped body (experiment of the A. F. Ioffe FTI on the aeroballistic route), were simulated [17]. In general, the acceptability of the developed computational tools and the turbulence model for forecasting the turbulent detached flow characteristics in a wake and in comparatively thin detached zones in near-wall regions was shown. The present paper lays emphasis on the estimation of the applicability of the developed numerical approach to the calculation of detached turbulent flows with the example of the supersonic flow around bodies with FSZ representing a combination of a disk and a cylinder with a flat end. An arrangement with two coaxial disks placed in front of and behind a finite-extension cylinder characterized by both a low wave drag and a low base drag is also considered.

Trajectory Analysis. The ballistic experiment on the investigation of the flow around the stepped model in question and its aerodynamic characteristics was performed on the Large ballistic installation of the A. I. Ioffe FTI [18]. The pressurized testing space can be filled with various gases at a pressure from 0.01 to 2 atm; the maximum velocity in using powder throwers [19] is 1800 m/s. The organized vibrations in the vertical plane form plane motion of models. Analysis of such motion considerably simplifies the procedure of trajectory investigation to find the dependence of the coefficients of aerodynamic forces on the angle of attack.

Experimental investigations of the model forms of stepped bodies were carried out at atmospheric pressure with a flight Reynolds number $\mathrm{Re} = 1.5 \cdot 10^6$.

The body under consideration — a cylinder with a coaxial thin disk — without a rear disk (Fig. 1a) features no significant stability and executes vibrations at the angle of attack within the limit of 2–4°. Assuming the change in the drag coefficient C_x to be weak in this range, we find its value by the method of determining the constant drag coefficient [20]. This method, also called the "tripoint" method, requires a knowledge of three x coordinates and two values of the time t sequentially at the registration posts. Using such a method, we obtain C_x as an arithmetic mean from the sequence of "tripoints."

Interference Measurements. At the center of the testing space, the cross-section of interferometry equipped with a shadow instrument transformed into a diffraction interferometer with a lentil-shaped field of length 200 mm in the longitudinal direction is located.

In testing the models of the bodies, instantaneous interferograms of the flow around the investigated body — a disk-cylinder arrangement (as well as shadowgrams with pulsed sources) — were obtained. The radial density profiles in the cross-sections of an axisymmetric streamlined body are recovered by the standard method [21]. In the given paper, the procedure of interference investigation is described. In the tuning field, ~60 equidistant bands perpendicular to the trajectory were set, and the dispersion of the path difference was assumed to be equal to 0.07 of the band. The field size was 200 mm.

The procedure within the framework of the algorithm [21] made it possible to set up a correspondence between bands on passing through the shock wave; the same technique permits establishing a correspondence between band numbers on the internal shock wave. The density estimation error characteristic of the field of supersonic flow around the bodies was determined.

The method of [21] relies in Shardin's approach. In [22], it was shown that such an algorithm does not lead to an appreciable accumulation of errors in internal ring zones. However, with decreasing sizes of the ring or near the deciphering cross-section axis, the error increased because of the decrease in the path on which the sought refractive index worked.

As a result, radial dimensionless density distributions were obtained and compared with the results of the numerical calculation. In considering a stepped body in flight, to decipher the density, cross-sections in the front separation zone between the protruding disk and the front end of the cylinder were chosen.

Features of the Computational Algorithm. The multiblock computational technologies of solving aerohydromechanics and heat transfer problems that have been developed in the last few decades are based on a priori given multiblock structured overlapping grids [23]. Their chief advantage is the accuracy of mapping of structural flow elements of different scales for whose trapping they are introduced.

In [24], the construction of multiblock computational technologies realized in the VP2/3 package as applied to the solution of problems of detached flow of an incompressible viscous liquid around bodies with vortex cells was discussed in detail. The approach to the solution of Reynolds equations is based on the known method of splitting between physical processes within the framework of the pressure correction procedure SIMPLEC [25]. The pressure correction equation is written instead of the continuity equation, which is justified for incompressible liquid flows. However, such a solution method is not unique. The artificial compressibility method [26] that permits constructing a marching solution method for a system of equations written in terms of the vector of dependent variables (velocity components, pressure) is widely used. The above method is in accord with the solution methods for equations for a viscous compressible gas that differ considerably from the pressure correction methods and have limitations at low Mach numbers.

In the 1980s, the construction of a generalized procedure of pressure correction equally applicable for incompressible liquid and compressible gas flows presented an urgent problem which was solved in a number of works (see, e.g., [27]). Separately, it should be noted that it is necessary to take into account the shocked flows that can be rather strong at supersonic flow velocities.

The previously developed [25, 26] pressure correction algorithms were based mainly on the application of multiblock grids. Moreover, the modern semiempirical turbulence models were not used in them. Successful attempts to construct a multiblock generalized pressure correction algorithm are associated with the calculations of reliefs with hollows [15, 16]. They are based on the monographs [24, 28, 29] as well as on the papers of Launder–Spalding, Menter et al., and Hellsten (see [13, 14, 28, 30]) devoted to the methodological aspects of turbulence models, especially of the shear stress transfer model, on whose application emphasis is laid in the given investigation. The methodological investigations [12] in which various discretization schemes are used are also worthy of note. An important feature of the developed computational algorithm for compressible turbulent shocked flows is its succession to the modelling of nonviscous flows.

The computational technology was formed in the period from 1983 to 2005 [12, 24, 28]. Navier–Stokes and Reynolds equations closed in the latter case by the MSST semiempirical differential model were solved by means of the finite-volume implicit procedure (predictor-corrector) of the SIMPLEC type with elements controlling the computational process. Recording of input equations in increments of dependent variables and schemes of various orders for approximating the right and left sides was realized. Upstream differences and additional damping in the implicit part, the Leonard QUICK scheme of convection terms of the explicit part along with the Rhi–Chow approach for interpret-

ing the pressure-velocity relation (with a relaxation coefficient equal to 0.1 determined from numerical experiments), as well as the method of incomplete matrix factorization were also introduced. The approach described above was evaluated in [31]. The given model presented a numerical simulation of an axisymmetric turbulent compressible air flow around a protruding coaxial disk in the range of limited variation of the Mach number from 0 to 0.7 (up to the formation of local supersonic zones and shock waves).

In the multiblock methodology, particular consideration was given to the construction of a compressible variant of SIMPLEC. It was also established by methodological calculations of shocked flows that for the computational process to be stable it is expedient to approximate the convective terms in the transfer equations by the Van Lear scheme, and this scheme should also be used to determine the density at the cell boundary rather than the central finite difference scheme [17]. It was also shown that the energy equation in the initial system of equations should be written and solved for the complete heat content. It is important to emphasize that the generalized approach widely uses the MSST model modified taking into account the correction for the streamline curvature — the Menter shear stress transfer model widely evaluated for calculating detached flows of incompressible liquid [13, 14]. In the given investigation, a comparative analysis of the results of calculations by this turbulence model and by the SA eddy viscosity model proposed by Spalart–Allmares [32] with Spalart and Shur corrections is performed.

Testing of the VP2/3 Package on the Problem of Sub- and Supersonic Flow around a Sphere. The flow around a sphere is calculated in the axisymmetric statement. Undoubtedly, in the subsonic range of variation of the Mach number the real flow pattern has a three-dimensional nonstationary character. However, as in the case of a circular cylinder, in the region of M = 1 and higher, the flow around the sphere is symmetrized, which permits considering the chosen statement of the problem to be correct.

The circular outer flow boundary of the computational domain is broken down into the input half on which fixed boundary conditions are set and the output part with soft boundary conditions on it. The outer boundary is situated at a long distances (35 calibres) from the body in order to avoid the influence on the flow in its vicinity. The uniform flow at the inlet into the domain models a flow in the working section of the wind tunnel with a turbulence level of 1.0%. The turbulence scale is determined by the honeycomb cell size equal to the cylinder diameter. On the symmetry axis the symmetry conditions and on the body the adhesion conditions are fulfilled.

Several multiblock grids differing in the number of computational cells, especially in their density in the wake, are considered. A series of calculations were made on a moderate three-level grid with 45,760 cells with their uniform distribution on the circular coordinate. In a wall layer of size 0.03, for correct mapping of the boundary layer, there are 30×320 cells with a near-wall mesh width of 10^{-4}. The second level of thickness 7 contains 160×160 cells, with the maximum radial mesh width not exceeding 0.1. Finally, the third level extends to the outer boundary and is split into 60×160 cells.

For data comparison, several more accurate calculations of the flow on a three-level grid with 100,480 cells were performed. As on the previous grid, the wall layer of cells of thickness 0.03 contained 30×320 cells with a near-wall mesh width of 10^{-4}. The second layer of thickness 7 contained 220×320 cells, and the third layer of size 35 contained 60×320 cells, with nodes crowding together on the circular coordinate towards the symmetry plane in the wake up to a value of 10^{-3}.

The Reynolds number determined from the uniform inlet flow velocity and the sphere diameter is taken to be equal to 10^6. The Mach number is varied from 0 to 4.

Analysis of Fig. 2a–d shows a quite satisfactory agreement between the presented results and the data of the aeroballistic experiment given in the Van Dyke atlas [33], with the given degree of turbulence of the incident flow being very low and equal to 10^{-3}. We should like to particularly emphasize the correct detection in the calculations of the positions of weak and strong shock waves, the latter being pendent, i.e., they are formed on the basis of a superposition of numerous compression waves from the shear layer at the boundary of the separation region.

The presented dependence of the drag coefficient on the Mach number of the incident flow clearly shows the critical phenomena connected with the increase in C_x in the transonic range of velocities (Fig. 2e). The discrepancy between calculations and experiments from monograph [34] concerns the subsonic range where the model of symmetric stationary flow around a sphere is not adequate. In the trans- and supersonic ranges of flow velocities, the agreement between calculations and experiments is quite satisfactory.

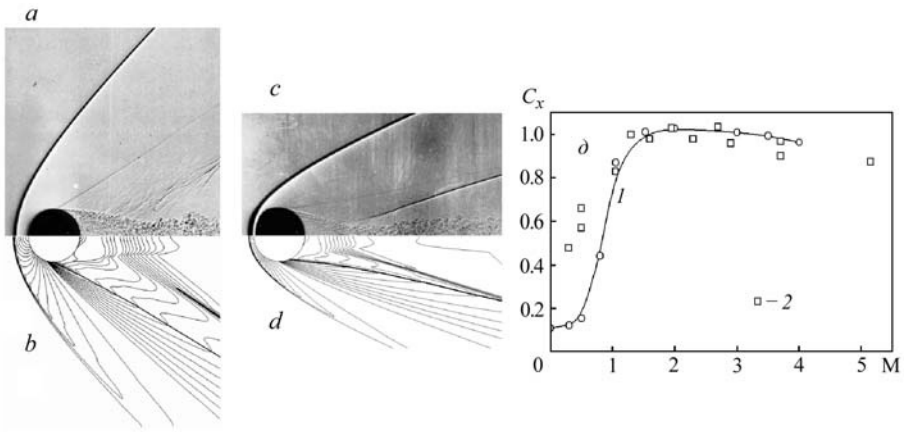

Fig. 2. Comparison of the shadow (a, c) and shock-wave patterns of the flow around a sphere ([32]) with shock waves plotted on the calculated pressure fields (b, d) at M = 1.53, Re = 10^5 (a, b) and at M = 3, Re = 10^6 (c, d); b) isobars from 0 to 0.75 were plotted with a step of 0.05, and from –0.15 to 0 with a step of 0.01; d) isobars from 0 to 0.9 were plotted with a step of 0.05 and from –0.06 to 0 with a step of 0.005; e) influence of the Mach number on the drag coefficient of the sphere [1) calculation, 2) experiment [33]].

Analysis of the Calculated and Experimental Results. Calculations of the supersonic axisymmetric flow around a stepped body (see Fig. 1a) were made within the framework of the methodological approach refined on the problem of flow around a sphere and a drop-shaped body [17]. The paper considers a cylindrical body of calibre 1 (the diameter was chosen as a characteristic size) and length λ (taken to be equal to 1) with thin coaxial disks placed at distances L and L_1. The disks had diameters d and d_1 and were positioned, respectively, in front of and behind the cylidner and connected to it by a thin jumper of diameter d_0 (was taken to be equal to 0.05). A system of cylindrical coordinates x, y, z with the center 0 in the middle of the front end of the cylinder was introduced. A uniform flow with Mach number varying from 1.5 to 4.15 is given on the left boundary situated at a distance of 10.5 from the cylinder end. The outlet boundary is situated at a distance of 27.5, and the upper boundary is distanced from the symmetry axis by 31.5. On both flow boundaries, the conditions for continuing the solution – the soft boundary conditions — are given. The turbulence energy of pulsations at the input to the computational domain complies with the conditions of the flight experiment ($k = 10^{-6}$), and the turbulent viscosity value is chosen to be smaller than the physical one. On the surface of the streamlined body, the adhesion conditions are given, and all washed walls are heat-insulated. To simplify the construction of the computational grid, we consider a cylinder with smoothed sharp edges, the rounding-off radius being taken to be equal to 0.01.

In the given case, the multiblock grid consists of six fragmentary structured intersecting grids: an external nonuniform Cartesian grid (Fig. 1b), a curvilinear O-type grid fit to the surface of a cylinder with rounded-off sharp edges and adjoining it, and four cylindrical grids near the two disks and the connecting jumper, respectively (Fig. 1c). The radial size of the O-type grid is 0.2 and it contained 165 × 48 cells. The Cartesian grid covered a rectangular region of size 38 by 31.5 calibres and contained 641 × 210 cells crowded together in the zone where the body was situated. The Cartesian grid width in the region of the cylinder was 0.01. The near-wall width was chosen to be equal to 10^{-4}.

The Reynolds number was taken to be equal to 10^6 and corresponded to the value in the aeroballistic experiment. The aim of the methodological part of the experiment performed was to carry out a comparative analysis of the results of calculations performed from the point of view of various turbulence models with the data of wind tunnel tests and the aeroballistic experiment.

On the basis of preliminary physical and numerical investigations [7–11, 35, 36], a rational wave-drag arrangement of a stepped disk-cylinder body with geometric sizes $L = 1.4$ and $d = 0.233$ is chosen. It should be noted that with such a gap L between the disk and the cylinder end a single separation zone is formed [35] and the super-

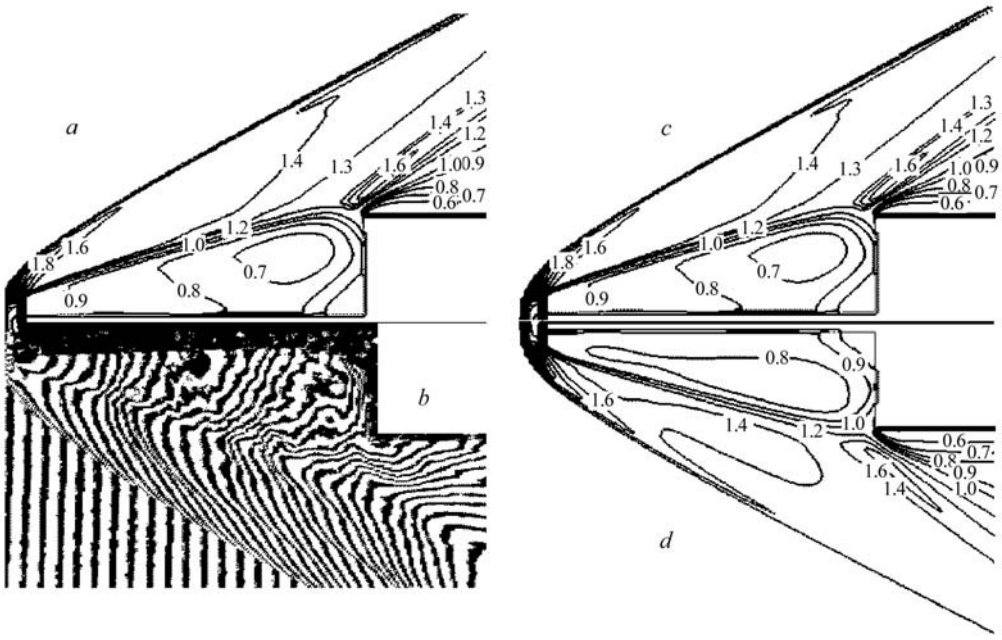

Fig. 3. Comparative analysis of the density fields calculated by different turbulence models [MSST (a, c); SA (d)] referred to the incident flow density and interferograms of the flow around a cylinder with a protruding disk (b). M = 2.35, Re = 10^6, L = 1.4, and d = 0.233.

sonic flow around the body is stable. Therefore, the use of a mathematical model based on the solution of stationary Reynolds equations closed by the differential equations of the turbulence model seems to be justified [14, 32].

Analysis of the Shock-Wave Pattern of the Flow around a Stepped Body at M = 2.35. As was established earlier [2, 4, 5, 7–10, 35, 36], the interaction of the supersonic air flow with a longitudinally oriented cylinder in the presence of a protruding disk leads to the formation of a bow shock in front of the body and the formation of a front separation zone in the gap between the disk and the cylinder end. In so doing, as was shown in [35], in the numerical simulation of the nonstationary process of supersonic flow incidence on a stepped body, the formation mechanism of the separation zone is explained solely by the nonviscous effects and the wave character of the transient process, and the stationary flow pattern results from the gradual attenuation of the rarefaction and compression waves propagating in the gap. As mentioned above, the nonviscous model of the medium turned out to be unacceptable because of the strong dependence of calculated results on the scheme (artificial) diffusion associated with the introduced discretization errors of convective terms of the approximation viscosity transfer equations and determined for first-order schemes of the given grid structure (by the grid widths and the slope of the grid lines) [8, 9]. We managed to improve the quality of modeling and increase the accuracy of numerical forecasts of the local and integral force characteristics by introducing, in the vicinity of the shear layer developing along the streamline separating the front separation zone and the external flow, a local a priori given subregion in which Reynolds equations closed by means of the second (convective) Prandtl model were solved [8–11]. Despite the success of using the developed zonal model, there is no doubt that it was constructed on the basis of a considerably simplified structure of the detached flow, on the assumption that the separating line is rectilinear and coincides with the line connecting the sharp edges of the disk and the cylinder. And, of course, it was based on a rather rough model of the shear layer whose subregion was given on the basis of empirical data on the development of free shear layers. Apparently, the applicability of such a zonal model is limited. In [11], it was noted that in the calculations by the zonal model the pressure field behind the shock wave and in the separation zone is reproduced with a fair accuracy and, therefore, the momentum exchange between the external flow and the circulating gas flow is mapped correctly. At the same time the energy exchange is modeled much worse. Outside the mixing layer the total energy transfer is determined by the scheme effects: the dissipation and the heat conductivity. It turned out that in using the Godunov scheme of the first order of approximation even on an oblique grid adapted to the flow structure the scheme dissipation coefficient exceeds the scheme heat conductivity coefficient. As a

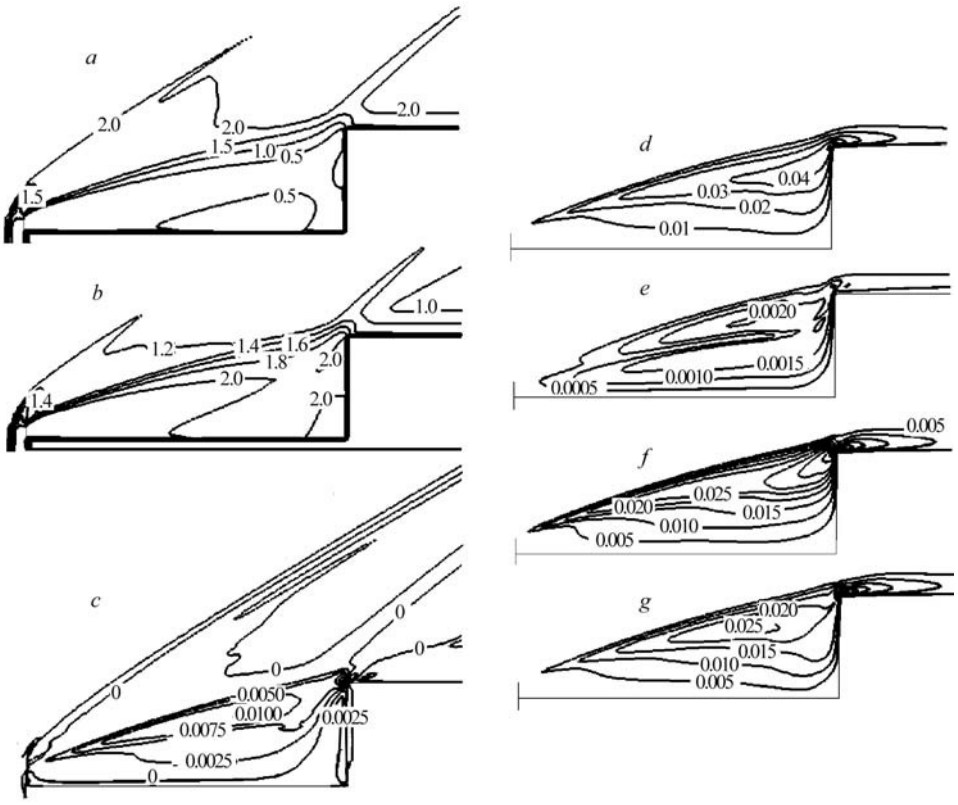

Fig. 4. Fields of the Mach number (a), the temperature referred to the incident flow temperature (b), turbulent friction $\overline{uv}$ (c), energy of turbulence (d), vortex viscosity (e), and Reynolds stress tensor components u'^2 (f) and v^2 (g). M = 2.35, Re = 10^6, L = 1.4, and d = 0.233.

consequence of this, in the separation zone energy storage occurs. In the calculations, the stagnation temperature inside the zone exceeded by 20% its value in the undisturbed flow.

Figure 3 compares the calculated density fields (referred to the air density of the incident flow) obtained by means of the MSST and SA models with the interferogram of the flow around a model of a stepped body flying on the aeroballistic route. As is seen from the presented patterns, the calculations forecast, to a fair accuracy, the form of the bow shock and the position of the shear layer developing at the boundary of the front separation zone. In general, there is a good agreement between the density fields calculated on the basis of the MSST-model with the correction for the streamline curvature and on the basis of a SA model. For instance, in the FSZ the formation of a rarefaction zone with the density minimum shifted to the front edge of the cylinder is noted, which agrees well with the position of the large-scale vortex center obtained earlier in [10]. It may be emphasized therewith that the MSST model forecasts a somewhat higher rarefaction level than the SA model. In the vicinity of the smoothed front edge of the cylinder an oblique shock wave arises, and turning the flow to the lateral surface leads to the appearance of a fan of rarefaction waves.

As follows from Fig. 4a, the flow in the FSZ is subsonic, and the maximum return flow velocities are observed in the middle vicinity of the connecting rod. Giving the boundary conditions of the heat-insulated walls on the washed surfaces leads to some heating in the large-scale vortex — the temperature exceeds twice the temperature level of the incident flow (Fig. 4b). It is interesting to analyze the turbulent friction field in Fig. 4c in order to estimate the acceptability of the proposed zonal model assumptions [8–11]. In general, it may be stated that the shear layer on the side of the external flow from the PSZ develops by a law close to linear. This is largely due to the fact that the external flow is practically nonviscous. Inside the zone, the shear layer has no clear boundary, although its thickening, judging from the level, 0.0075, is also close to linear thickening, except for the vicinity of the center of the large-scale vortex. As is seen from Fig. 4d, the turbulence energy increases gradually as the vortex moves along the reference line

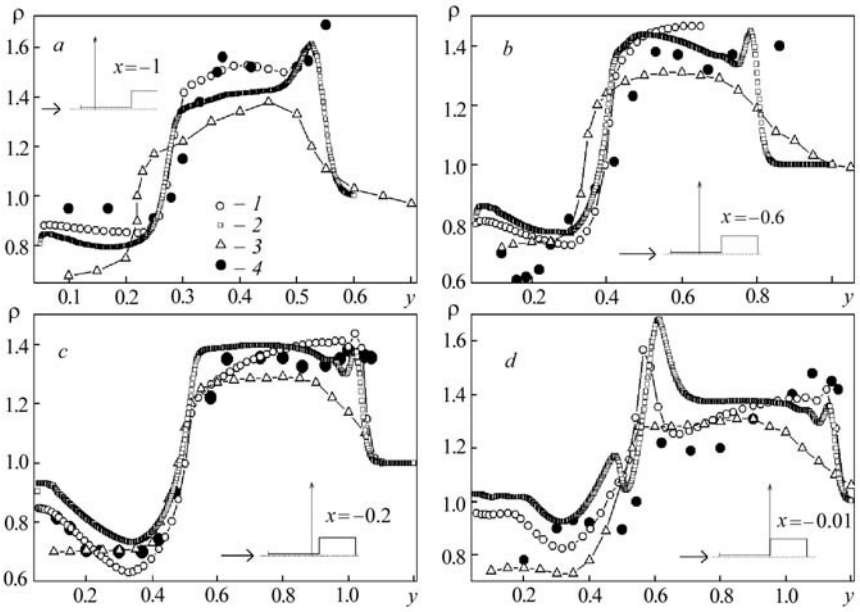

Fig. 5. Comparison of calculated (1–3) and experimental (4) relative density ρ profiles in FSZ cross sections: a) $x = -1$; b) –0.6; c) –0.2; d) –0.1; 1) MSST; 2) SA; 3) zonal model [7–11]; 4) experiment. M = 2.35; Re = $1.5 \cdot 10^6$; $L = 1.4$, and $d = 0.233$.

connecting the disk and cylinder edges. The behavior of the vortex viscosity coefficient (Fig. 4e) on the major portion of the reference line is analogous, which complies with the linear viscosity increase law used in the convective Prandtl model [8–11]. It is interesting to note the difference in the fields u'^2 and v'^2, with the maximum of the latter characteristic practically coinciding with the center of the large-scale vortex.

Comparison of the Density Profiles in the Front Separation Zone. As mentioned earlier, the interferogram shown in Fig. 3b was obtained on a grating shearing interferometer on the basis of an IAB-451 shadow device. For beam splitters, gratings of frequency 75 grooves/mm were used and at an OGM-20694.3 laser wavelength of 694.3 nm and a focal length of the lenses of 1918 mm the shift of the interfering wave fronts was 100 mm. The investigated inhomogeneity in the meridional section occupied an area of 60×100 mm^2.

In constructing the path difference function by the interference pattern of the turbulent zone, we used a priori information on the flow around a stepped body. The direction of variation of the path difference near the extrema and the bend lines of the wave surface of the probing light was determined proceeding from the fact that the FSZ separated by the mixing layer is a low-pressure region with respect to the shock-compressed layer.

It should be noted that the interference method compares unfavorably with the schlieren method as to the sensitivity to the pulsation transfer and leads to the rolling-off of the input spectrum for small-scale pulsations. At the same time pulsations of the turbulent region boundary (mixing layer, wake) are transferred by the interferometer with a relatively large contribution compared to internal pulsations. It has been shown with the example of the turbulent wake behind a sphere that the output signal (deformation of bands) from boundary pulsations exceeds 10 times the signal from pulsations in the internal volume. In using the schlieren method, this signal ratio is 0.125, and for the glow point method it is 0.033.

The disordered pattern of bands in the FSZ (Fig. 3b) on the processed interferograms is largely due to the pulsations of the mixing layer boundaries. Using the measurement data for the band coordinates in the cross-sections on either side of the inhomogeneity axis, we constructed path differences smoothed in the limit of 0.3–0.5 of the band with respect to the middle curves. To check the stability of the inverse problem solution on the given inhomogeneity, we introduced 10 times the largest possible error of the path difference distributed along the radius of the cross-section in accordance with the law of random numbers. The mean density determination error is about 4% in the shock-compressed region and 10% in the FSZ.

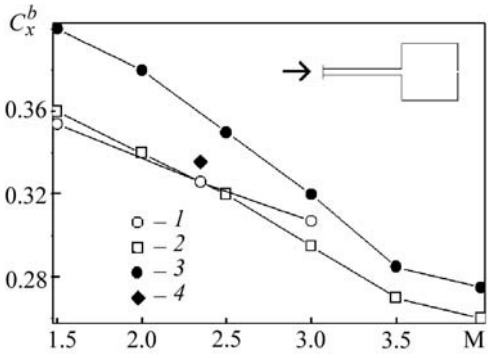

Fig. 6. Comparison of various calculated and experimental dependences of C_x^b (M) (Re = 10^6, L = 1.4, and d = 0.233): 1) MSST; 2) zonal model [10]; 3) wind tunnel tests [10]; 4) aeroballistic experiment.

Figure 5 compares the calculated and experimental relative density profiles in the FSZ cross-sections in a supersonic flow (M = 2.35) around a stepped body with L = 1.4 and d = 0.233. The solutions of MSST — (curve 1) and SA — closed (curve 2) Reynolds equations are complemented with forecasts by the zonal model (curves 3) [7–11] and are superimposed on the interferometric data determined on the basis of the aeroballistic experiment (4).

As was noted in [11], the lower value of the density behind the shock wave is explained by its spreading in the calculation by the zonal method. On the contrary, the calculation of the detached flow around a stepped body with the use of the generalized implicit pressure correction procedure and differential turbulence models demonstrates a good mapping of the bow shock position. As in the numerical simulation of the supersonic flow around a drop-shaped body [17], in the given case the density profiles in the shocked-compressed layer near the body between the FSZ and the bow shock are reproduced fairly accurately. At the same time the discrepancies between forecasts by the zonal model and experimental data in this zone are very wide.

The shear layer position is easily determined by the large density gradient. It is easy to see that the shear layer behind the disk up to the middle of the FSZ is positioned somewhat higher than the reference line connecting the disk and cylinder edges. Therefore, forecasts by the zonal model differ somewhat from the results of calculations by the differential turbulence model and the experimental data that agree well with each other (Fig. 5a, b). In the section close to the center of the large-scale vortex (Fig. 5c), in the zone where the shear layer is situated, all calculated curves are in good agreement with experimental points. The widest discrepancies between the results of numerical and physical simulations, despite their qualitative similarity, are observed near the cylinder end x = –0.01 (Fig. 5d), although deviations do not exceed the density measurement error in the separation zone.

The FSZ density forecast by the differential turbulence model, as was supposed in [11], is in a better agreement with interferometric data than forecasts by the zonal model. The maximum rarefaction in the connecting jumper zone turns out to be of the order of 0.6–0.8 of the density level of the incident flow.

Comparing the results of calculations by the MSST and SA models with empirical data (Fig. 5), we can note a certain advantage of the Menter shear stress transfer model (deviations from forecasts by their model from experimental data are somewhat smaller than for the SA model).

In general, the conclusion drawn in [17] that the MSST differential turbulence model is acceptable for calculating the local characteristics of the supersonic detached flow around drop-shaped bodies is extended to stepped bodies with separation zones organized in front of them. The MSST model has certain advantages over the SA model.

Comparison of Calculated and Experimental Wave Drag Coefficients of a Cylinder with a Protruding Disk. We determined the drag coefficient C_x by measuring the decrease in the model velocity in flight on the ballistic installation without the angle of attack. Subtracting from it the base drag coefficient C_x^d corresponding to the base pressure measurements, we obtained the estimate of the wave drag of the model C_x^b. In the aeroballistic experiment C_x^b = 0.334 [11].

In [10], we presented the results of the experimental investigation in a supersonic wind tunnel with a working section of rectangular cross-section (0.12 × 0.15 m^2) with changeable nozzle linings (M = 1.96, 2.9, 4.15). The minimum Reynolds number constructed by the cylinder diameter and the flow parameters in the working section is of the

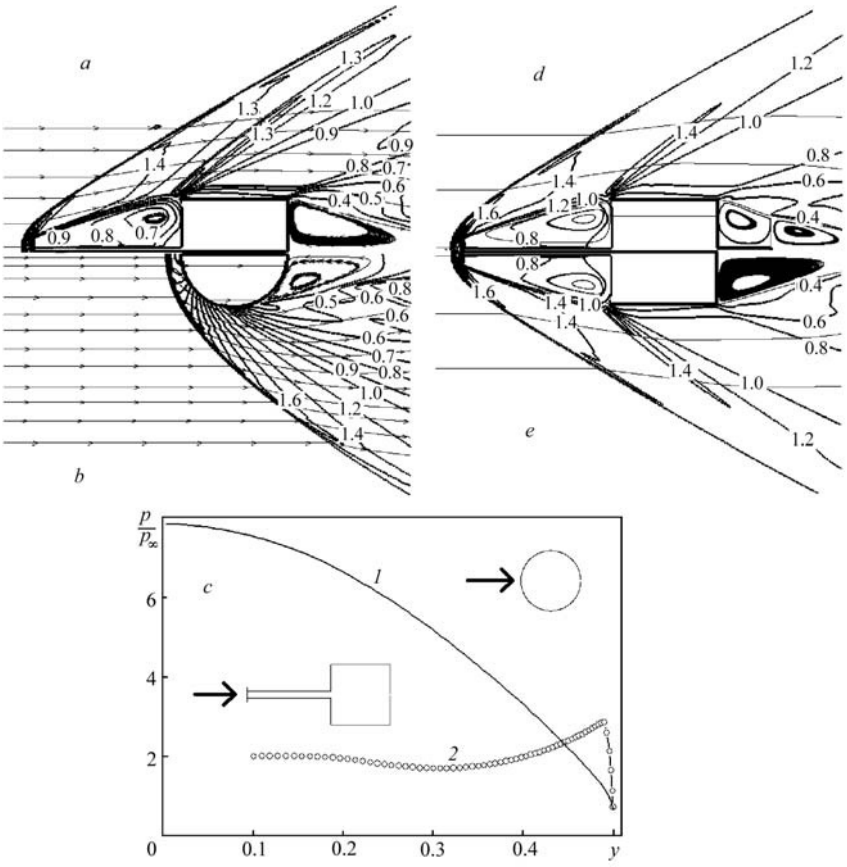

Fig. 7. Comparison of the relative density fields for a cylinder with a protruding disk (a, d), a sphere (b), and a disk–cylinder–disk arrangement (e), as well as of the relative pressure distributions (c) over the sphere contour (1) and the end of a cylinder with a front disk (2). M = 2.35, Re = 10^6, L = 1.4, d = 0.233, L_1 = 0.5, d_1 = 0.66.

order of 10^6. The blocking-up of the working section of the tunnel by the model did not exceed 3%. As a result of statistical tests of the models of stepped bodies on a strain-gauge three-component balance, the wave drag coefficient C_x^b depending on the characteristic parameters d, L, M was determined. The relative error of C_x^b determination was about 5%.

Figure 6 compares the calculated and experimental results on the wave drag coefficient C_x^b depending on the incident flow Mach number. In so doing, mathematical models of various levels and different experimental methods were used. Noteworthily, there is a good agreement between the results, which points, first of all, to a good acceptability of the approach based on the MSST differential turbulence model and multiblock computational technologies. However, a similar good agreement with experimental data on integral force loads determined by the considerably simplified zonal model also looks interesting. The reason, as was noted earlier, is the successful combination of the characteristic features of the computational and physical models for the chosen disk-cylinder arrangement (L = 1.4). Evidently, for other geometrical shapes and sizes and for other regime parameters such a combination of models will be lost, which will lead to serious deviations of forecasts from experimental data.

Analysis of the Supersonic Flow around a Sphere and Cylinders with Front and Rear Coaxial Disks. The comparison of the supersonic flow patterns around bodies of different shapes at M = 2.35 and Re = 10^6, as well as of the integral force loads acting on them, is presented in Fig. 7 and Table 1.

As is known [34], the sphere is a bluff body. The bow shock formation in front of such bodies (Fig. 7b) leads to a manifold increase in the static pressure distributed over the contour as compared to the incident flow pressure (Fig. 7c). Placing a small-diameter disk in front of a bluff body (flat-end cylinder) leads to a displacement of the

TABLE 1. Comparison of the Integral Force Characteristics in the Supersonic Flow around a Sphere, a Cylinder with a Protruding Disk (L = 1.4, d = 0.233), and Cylinders with Coaxial Disks (L = 1.4, d = 0.233, L_1 = 0.5, d_1 = var) at M = 2.35 and Re = 10^6

Body	C_x	C_x^b	C_x^d
Sphere	1.017	0.850	0.162
Disk–cylinder	0.486	0.325	0.153
Disk–cylinder–disk			
d_1 = 0.55	0.495	0.327	0.160
d_1 = 0.60	0.488	0.327	0.153
d_1 = 0.66	0.479	0.327	0.144
d_1 = 0.70	0.476	0.328	0.140
d_1 = 0.75	0.472	0.327	0.137
d_1 = 0.80	0.467	0.327	0.132
d_1 = 0.85	0.474	0.327	0.135

bow shock from the body located in the wake behind the disk (Fig. 7a). Since the disk area is much smaller than the area of the cylinder end, the load on it is also smaller than in the supersonic flow around a single cylinder. The load on a cylinder with a protruding disk consists of the disk load and the load on the cylinder with an FSZ. As is seen from Fig. 7c, the end pressure is almost constant in this case and is only twice higher than the incident flow pressure. On the whole, the wave drag of a cylinder with a protruding disk is almost three times smaller than that of a sphere at an approximately equal base pressure (see Table 1).

As was shown in [36, 37], in the axisymmetric incompressible liquid flow around a cylinder with coaxial disks, placing the disk in the base part markedly decreases the base drag of the body. In the base investigation, we made an attempt to analyze the influence of the rear disk on the supersonic flow around the disk–cylinder–disk arrangement, the bow being chosen from the minimum wave drag condition, i.e., with L = 1.4, d = 0.233. As follows from Fig. 7d, e, the flow pattern in the FSZ with a rear disk remains unaltered since the wave drag of the body remains practically the same. Of course, the rear disk position should be chosen from the base drag minimization condition. Here the distance L_1 is given by the value 0.5, and the disk diameter d_1 is varied over the 0.55–0.85 range, As follows from Table 1, at d_1 = 0.8 the base drag of the cylinder is minimum and about 12% lower than in the case of the absence of a rear disk.

CONCLUSIONS

1. The good agreement between the results of the numerical and physical simulation of the flow around a cylinder with a protruding disk points to the adequacy of the used computational approach based on the solution of stationary Reynolds and energy equations with the aid of multiblock computational technologies and the generalized pressure correction procedure.

2. On the basis of comparison with experimental results and numerical forecasts of the local and integral characteristics of the flow around a cylinder with a protruding disk by the Spalart–Allmares model, the acceptability of the Menter shear stress transfer model (modified with account for the streamline curvature correction) has been justified. This model previously tested for incompressible detached flows [12, 14] is applicable for calculating organized detached flows in a wide range of variation of the incident flow Mach numbers — from 1.5 to 4.

3. In turn, the agreement between the numerical forecasts and the measurement data on the local characteristics and integral estimates of the motion drag of stepped bodies points to the adequacy of the aerophysical methods based on the processing of data of the aeroballistic experiment.

4. Placing a rear disk behind a cylinder with a protruding front disk makes it possible to decrease the base drag of the arrangement, and there exists an optimal parameter of the disk at which C_x^d is minimal. At a cylinder length equal to 1, L = 1.4, d = 0.233, L_1 = 0.5, M = 2.35, and Re = 10^6 the optimal diameter d_1 = 0.8 and the base drag decreases by 12% compared to the variant without a rear disk.

This work was supported by the Russian Foundation for Basic Research (projects No. 10-08-00510 and 08-01-00059).

NOTATION

a, velocity of sound, m/s; C_x, C_x^b, C_x^d, motion, wave, and base drag coefficients; D, cylinder diameter, m; d, d_1, diameter of the front and the rear disk, in fractions of D; d_0, diameter of the connecting rod, in fractions of D; k, energy of turbulent pulsations, in fractions of U^2; L, L_1, protrusion of the front and the rear disk, in fractions of D; M, Mach number, M = U/a; p, static pressure, fractions of $\rho_\infty U^2$; Re, Reynolds number, Re = $\rho_\infty UD/\mu$; T, temperature; t, time, s; U, incident flow velocity, m/s; u'^2, $\overline{uv}$, v^2, averaged Reynolds stress tensor components, in fractions of U^2; x, y, longitudinal and transverse coordinates, in fractions of D; λ, cylinder extension, in fractions of D; μ, dynamic viscosity coefficient, kg/(m·s); ρ_∞, incident flow density, kg/m^3; ρ, relative density of air, in fractions of ρ_∞. Subscript: ∞, incident flow parameters.

REFERENCES

1. P. Chang, *Separation of Flows* [Russian translation], Vol. 2, Mir, Moscow (1973).
2. I. A. Belov, *Interaction of Nonuniform Flows with Barriers* [in Russian], Mashinostroenie, Leningrad (1983).
3. I. A. Belov and S. A. Isaev, Numerical simulation of the supersonic flow past bodies of revolution with a front separation zone, *Pis'ma Zh. Tekh. Fiz.*, **6**, Issue 10, 608–611 (1980).
4. I. A. Belov and E. F. Zhigalko, Front separation zone in the flow past a blunt body (computational model), *Izv. Akad. Nauk SSSR, Mekh. Zhidk. Gaza*, No. 1, 184–187 (1981).
5. I. A. Belov and E. F. Zhigalko, Extreme characteristics of the resistance of a cylinder equipped at the front with a disk in a supersonic flow (computational model), *Prikl. Mekh. Tekh. Fiz.*, No. 6, 38–41 (1981).
6. A. N. Lyubimov, N. M. Tyumnev, and G. I. Khug, *Methods for Investigating Gas Flows and Determining the Aerodynamic Characteristics of Axisymmetric Bodies* [in Russian], Nauka, Moscow (1995).
7. I. A. Belov, S. A. Isaev, V. N. Konovalov, and A. Yu. Mitin, Estimation of the wave resistance of bodies of revolution with a front separation zone in a supersonic flow, *Izv. SO Akad. Nauk SSSR, Ser. Tekh. Nauk*, No. 4, Issue 1, 47–51 (1985).
8. I. A. Belov, S. A. Isaev, V. N. Konovalov, and A. Yu. Mitin, Application of the concept of an ideal fluid for calculating the separation flow past blunt bodies with account for the turbulent shear layer at the boundary of the separation region, *Pis'ma Zh. Tekh. Fiz.*, **10**, Issue 20, 1217–1220 (1984).
9. I. A. Belov, S. A. Isaev, and A. Yu. Mitin, Calculation of detached flows from the viewpoint of the ideal fluid model with allowance for the turbulent shear layer on the boundary of the separation reigon, *Inzh.-Fiz. Zh.*, **51**, No. 4, 555–563 (1986).
10. I. A. Belov, S. A. Isaev, V. N. Konovalov, and A. Yu. Mitin, Modeling of large-scale vortex structures in a turbulent supersonic flow past a blunt body, *Izv. SO Akad. Nauk SSSR, Ser. Tekh. Nauk*, No. 15, Issue 4, 101–107 (1987).
11. A. Yu. Mitin and A. N. Mikhalev, Comparison of the results of interferential and numerical determination of the flow density in the separation zone, *Inzh.-Fiz. Zh.*, **49**, No. 11, 769–773 (1985).
12. Yu. A. Bystrov, S. A. Isaev, N. A. Kudryavtsev, and A. I. Leontiev, *Numerical Simulation of the Vortex-Assisted Intensification of the Heat Transfer in Tube Banks* [in Russian], Sudostroenie, St. Petersburg (2005).
13. F. R. Menter, Zonal two equation k–ω turbulence models for aerodynamic flows, *AIAA Paper*, 93–2906 (1993).
14. F. R. Menter, M. Kuntz, and R. Langtry, Ten years of industrial experience with the SST turbulence model, in: K. Hajalic, Y. Nogano, M. Tummers (Eds.), *Turbulence, Heat and Mass Transfer 4*, Begell House, Inc. (2003).
15. S. A. Isaev, Numerical simulation of the vortex heat transfer in a sub- and supersonic flow past dimpled reliefs with the aid of multiblock computational technologies, in: *Problems of Gas Dynamics and Heat/Mass Transfer in Power Plants, Proc. XV School-Seminar of Young Scientists and Specialists under the guidance of Academician A. I. Leontiev*, Vol. 1, MÉI, Moscow (2005), pp. 7–12.

16. A. I. Leontiev, S. A. Isaev, and G. S. Sadovnikov, Numerical simulation of the decrease in heat loads in a super- and hypersonic flow past a plane wall with trenches and dimples, *Teplovye Protsessy v Fizike*, No. 9, 362–366 (2009).
17. S. A. Isaev, A. N. Mikhalev, A. G. Sudakov, and A. E. Usachov, Modeling of the turbulent flow past a drop-shaped body with a conical skirt, *Zh. Tekh. Fiz.*, **77**, Issue 8, 29–35 (2007).
18. I. V. Basargin, I. M. Dement'ev, and G. I. Mishin, A proving ground for aerodynamic investigations, in: *Aerophysical Investigations of Supersonic Flows* [in Russian], Nauka, Leningrad–Moscow (1967), pp. 168–178.
19. I. M. Dement'ev and N. P. Mende, *Laboratory Accelerators for Aerodynamic Investigations on Ballistic Plants*, Preprint No. 831 of the A. F. Ioffe Physical-Technical Institute, Leningrad (1981).
20. N. P. Mende, On one method of determining nonlinear aerodynamic forces and moments, in: *Physicogasdynamical Ballistic Investigations* [in Russian], Leningrad (1980), pp. 200–223.
21. N. P. Mende and Yu. E. Shtrengel', *An Algorithm for Reconstructing the Gas Density in an Axisymmetric Flow from the Data of Interference Measurements with Error Estimation*, Preprint No. 1564 of the A. F. Ioffe Physical-Technical Institute, Leningrad (1991).
22. N. P. Mende, *Computational Tomography: on the Accumulation of Path Difference Errors in the Methods with Layer-by-Layer Splitting of an Object*, Preprint No. 1350 of the A. F. Ioffe Physical-Technical Institute, Leningrad (1980).
23. S. A. Isaev, A. G. Sudakov, P. A. Baranov, A. E. Usachov, S. V. Strizhak, Ya. K. Lokhanskii, and S. V. Guvernyuk, Development, verification, and application of the parallelized open-type VP2/3 package based on multiblock computational technologies for solving fundamental, applied, and operational problems of aeromechanics and thermal physics, *Vestn. YuUrGU*, *Ser. "Mat. Modelir. Programmir.,"* No. 17 (150), Issue 3, 59–72 (2009).
24. A. V. Ermishin and S. A. Isaev (Eds.), *Control of the Flow Past Bodies with Vortex Cells as Applied to Flying Vehicles of Integral Arrangement* (*Numerical and Physical Simulation*) [in Russian], MGU, Moscow (2003).
25. J. H. Ferziger and M. Peric, *Computational Methods for Fluid Dynamics*, Berlin, Heidelberg (1999).
26. K. C. Karki and S. V. Patankar, Pressure-based calculation procedure for viscous flows at all speed in arbitrary configuration, *AIAA J.*, **27**, 1167–1174 (1989).
27. Y. G. Lai, R. M. C. So, and A. J. Przekwas, Turbulent transonic flow simulation using a pressure-based method, *Int. J. Eng. Sci.*, **33**, No. 4, 469–483 (1995).
28. I. A. Belov, S. A. Isaev, and V. A. Korobkov, *Problems and Methods of Calculating Incompressible Detached Fluid Flows* [in Russian], Sudostroenie, Leningrad (1989).
29. I. A. Belov and S. A. Isaev, *Modeling of Turbulent Flows: Textbook* [in Russian], BGTU, St. Petersburg (2001).
30. A. Hellsten, Some improvements in Menter's k–ω turbulence model, *AIAA Paper*, 98-2554 (1998).
31. V. K. Bobyshev and S. A. Isaev, Numerical investigation of the effect of compressibility on the mechanism of decreasing the motion drag of a cylinder with organized separation zones in a turbulent viscous gas flow, *Inzh.-Fiz. Zh.*, **71**, No. 4, 606–612 (1998).
32. P. R. Spalart and S. R. Allmares, A one-equation turbulence model for aerodynamic flows, *AIAA Paper*, 92-0439 (1992).
33. M. Van Dyke, An Album of Fluid Motion [Russian translation], Mir, Moscow (1986).
34. K. P. Petrov, *Aerodynamics of Bodies of Simplest Shapes* [in Russian], Faktorial, Moscow (1998).
35. I. A. Belov, I. M. Dement'ev, S. A. Isaev, et al., *Modeling of a Supersonic Flow Past Bodies of Revolution with a Front Separation Zone*, Preprint No. 1033 of the A. F. Ioffe Physical-Technical Institute, Leningrad (1986).
36. I. A. Belov, I. M. Dement'ev, S. A. Isaev, et al., *Analysis of the Results and Methodological Justification of the Modeling of a Flow Past Bodies with a Front Separation Zone*, Preprint No. 1353 of the A. F. Ioffe Physical-Technical Institute, Leningrad (1989).
37. S. A. Isaev, Numerical simulation of the axisymmetric low-velocity flow around a cylinder with coaxial disks, *Inzh.-Fiz. Zh.*, **68**, No. 1, 19–25 (1995).